JOURNAL OF APPLIED ELECTROCHEMISTRY **18** (1988) 710–714

Enhanced mass transfer to a rotating cylinder electrode with axial flow

A. EKLUND, D. SIMONSSON

Department of Applied Electrochemistry and Corrosion Science, The Royal Institute of Technology, S-100 44 Stockholm, Sweden

Received 1 December 1987; revised 17 March 1988

A study of the rotating concentric cylindrical electrode has been made, in which the enhanced mass transfer rate by turbulence promotors to a smooth cylinder has been measured. When a special polypropene cloth was applied in the annulus an increase in the Sherwood number was detected, up to six times the value for a smooth cylinder at low Taylor numbers.

Nomenclature

A	electrode area, πdl (m^2)
C_0	bulk concentration ($mol\,m^{-3}$)
D	diffusion coefficient ($m^2\,s^{-1}$)
e	annular gap, $R - r$ (m)
F	Faraday's constant, 96487 ($A\,s\,mol^{-1}$)
I_l	limiting current (A)
k_l	mass transfer coefficient, I_l/nFC_0A ($m\,s^{-1}$)
l	electrode height (m)
n	number of electrons
r, R	radius of inner and outer cylinder (m)
u	axial liquid velocity ($m\,s^{-1}$)
ω	angular velocity ($rad\,s^{-1}$)
ν	kinematic viscosity ($m^2\,s^{-1}$)
ϱ	liquid density ($kg\,m^{-3}$)

Dimensionless numbers

Re_a	axial Reynolds number $2eu/\nu$
Re_ω	rotational Reynolds number $2r^2\omega/\nu$
Sc	Schmidt number ν/D
Sh^*	rotational Sherwood number $2rk_l/D$
Sh	combined flow Sherwood number $2ek_l/D$
St	Stanton number $Sh/Re_\omega/Sc$
Ta	Taylor number $= r\omega e/\nu(e/r)^{1/2}$
a, b, c	power indices

1. Introduction

Studies on the rotating cylindrical electrode (RCE), particularly the mass transfer rate to the electrode surface and various possible and effective applications, have been reviewed by Gabe and Walsh [1] and Pickett [2]. One of these applications is the rotating inner electrode in a concentric cylindrical cell [3].

The advantages of the rotating concentric cylindrical inner electrode (RCCE) may be summarized in terms of high mass transfer rates in turbulent flow, even at low rotation rates, and efficient mixing of solution in a relatively small cell volume.

The mass transfer behaviour of a smooth RCE was first studied by Eisenberg *et al.* [4, 5] who proposed a dimensionles correlation of the form $St = 0.079 \times Re_\omega^{-0.30} Sc^{-0.644}$. Subsequent studies have given essentially the same results [1, 6] with only small deviations in the indices a, b, c.

An extensive study of mass transfer to a rotating concentric inner cylinder was made by Coeuret *et al.* [7–9] for smooth cylinders in an annulus with axial flow. They considered the relation between axial and rotational flow for $Ta < 600$ and separated their effects in a correlation of the type

$$Sh = aRe_a^b Ta^c Sc^d$$

For $25 < Re_a < 300$, $a = 0.38$, $b = 0$, $c = 0.49$ and $d = 0.34$. For $Re_a > 300$, $a = 0.12$, $b = 0.34$, $c = 0.40$ and $d = 0.35$.

An increase in the mass transport rate for an electrochemical process can be achieved by changing either the solution parameters, by changing the temperature and concentration, or the geometrical parameters of the electrode (surface area, the ratio between annulus and inner radius, etc.).

One effective method of enhancing mass transfer is to roughen the electrode surface by machining patterns to provide increased surface area and agitation [10].

Recently, several investigations of the behaviour of expanded metal electrodes have been published. Expanded metal electrodes present a higher specific area and promote turbulence in the electrolyte flowing over them [10]. In this work the effects of similar turbulence promotors on the mass transfer rate to a rotating concentric cylindrical electrode were measured. Three different flow obstacles were tested and the consequent mass transfer rates measured and correlated with parameters characterizing the flow. By comparison with the smooth cylinder, degrees of enhancement have been calculated.

2. Experimental details

The rotating concentric cylindrical cell used in the experiments and the flow scheme are shown in Fig. 1.

0021-891X/88 $03.00 + .12

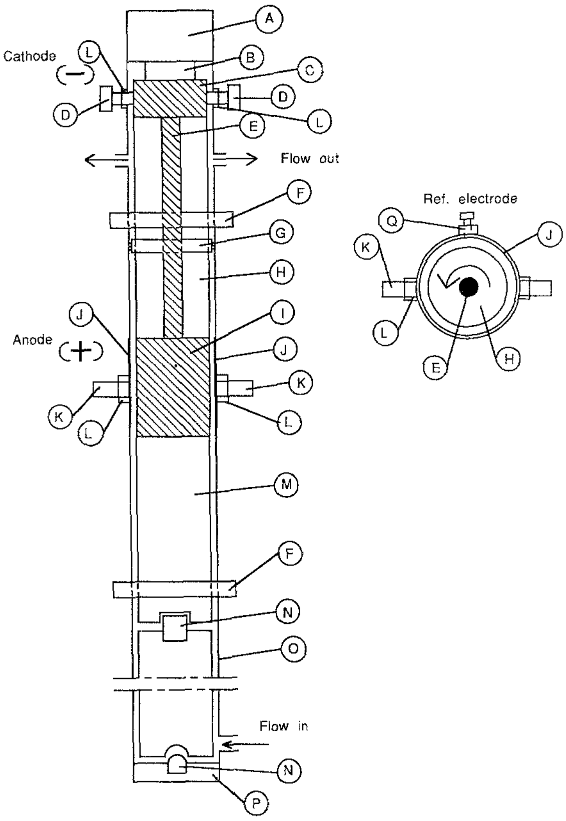

Fig. 1. Schematic drawing of the rotating cylinder electrode assembly. (A) Electric drive motor; (B) Teflon connections; (C) upper nickel cylinder; (D) silver electrical connectors; (E) inner nickel cylinder; (F) plexiglass joint; (G) Teflon steering; (H) inner plexiglass cylinder; (I) nickel cathode; (J) nickel anode: (K) nickel connection; (L) plexiglass screwholder; (M) plexiglass rod; (N) Teflon steering; (O) outer plexiglass cylinder; (P) plexiglass bottom sealing; (Q) reference electrode.

The essential elements of the cell are a stationary outer cylinder made of plexiglass, in which the anode of nickel was embedded, and an inner rotating cylinder on which the cathode, made of nickel, was mounted at a height of 10 cm above the lower end.

The anode was 30.2 mm high and the inner diameter was 31.9 mm. A notch was made in the middle of the anode with four holes uniformly placed around the periphery. This was to ensure a good connection between the electrolyte and the reference electrode (Hg/HgO). Through the outer cylinder wall two holes were made for electrical connections from the anode to a potentiostat (PAR, model 362). The cathode was 30.2 mm high and its outer diameter was 25.2 mm. Thus the annular gap, e, formed by the cylinders was 3.35 mm. The cathode was situated at the same height as the anode to ensure a uniform current distribution. The cathode was connected to the potentiostat through a nickel rod inside an inner plexiglass cylinder above the cathode to an upper nickel cylinder, which was in electrical contact with two silver connectors.

The liquid was fed through a single hole at the bottom of the outer cylinder and was exhausted through two holes below the upper nickel cylinder. The electrolyte was continuously recirculated by a centrifugal pump through a reservoir, where the temperature was measured and controlled, and through flow meters. Except for the anode and the cathode, no metallic part was in contact with the liquid.

The upper end of the cylinder was coupled to a d.c. electrical motor, the velocity of which could be varied. The angular velocity of the inner cylinder was measured by means of a digital optical tachometer sensing the light reflected from a small piece of reflecting material placed on the cylinder itself.

The electrolyte used was an aqueous solution of 1.0 M KOH supporting a mixture of 0.0025 M $K_3Fe(CN)_6$ and 0.025 M $K_4Fe(CN)_6 \cdot 3H_2O$. The high ratio (10 : 1) between the concentrations of ferro- and ferricyanide allow the reaction to be diffusion limited at the cathode only. The required amounts of the salts were weighed and the true ferricyanide concentration was determined by a back titration of iodine with $Na_2S_2O_3$.

The mass transfer rate of ferricyanide ions to the rotating cylinder electrode was determined from the limiting current density. All experimental series were run in duplicate. The maximum deviation between the two measurements at the same conditions was less than 5%. Reported values are mean values.

The diffusion coefficient of the ferricyanide ion in the solution was calculated from the well-known relation of Nernst–Einstein and from the literature [11]. The kinematic viscosity for the potassium hydroxide solution was taken from the literature [12] and recalculated to the actual temperature (22° C). The calculated values were $D = 0.764 \times 10^{-9}$ and $\nu = 1.019 \times 10^{-6} \mathrm{m^2 s^{-1}}$. The cylinder rotation speed varied between 0.5 and 27.0 Hz equivalent to a peripheral velocity of 0.04–2.15 $\mathrm{m\,s^{-1}}$ and the axial flow rate varied between 6.48 and 87.81 $\mathrm{l\,h^{-1}}$ (0.0064 to 0.086 $\mathrm{m\,s^{-1}}$).

The flow obstacles used to enhance mass transfer were made of polypropene, which is resistant in potassium hydroxide for long periods. The flow obstacle termed 'grid' had a 1 cm spacing between the threads in a squared appearance. The grid was 1 mm thick, so that when it was placed in the annulus it needed three consecutive layers, formed to a cylinder, to fill the annulus. The net had 1.0 mm spacing between the threads, also in a squared appearance. The net was 1.0 mm thick and three consecutive layers, formed to a cylinder, were used to fill the annulus.

The cloth was a specially made carpet weave from Engtex (Y 840925 B) with a thickness of 3.5 mm and a weight of 404 $\mathrm{g\,m^{-2}}$. The cloth was fastened on the outer electrode and it filled the whole annulus and brushed on the inner rotating electrode.

3. Results

The overall mass transfer rate was first measured for the case with no rotation of the electrode, when the electrolyte flows axially in the annulus formed by the two cylinders. This situation has been extensively studied in the literature, particularly by Ross and Wragg [13] whose experimental data for the laminar flow regime were described by the two correlations

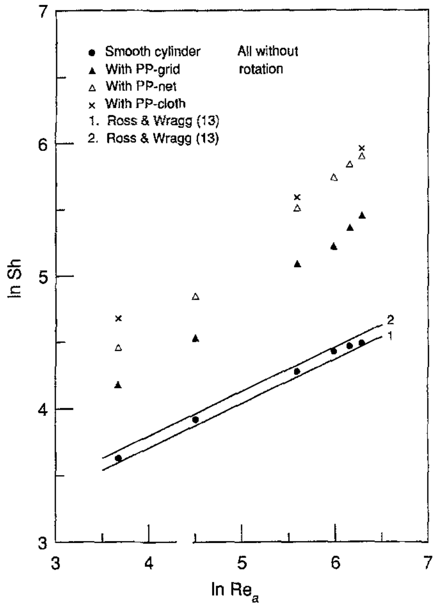

Fig. 2. Mass transfer with axial flow alone ($Sc = 1334$). Comparison of the effects of different turbulence promotors and with correlations from the literature (solid lines).

shown graphically in Fig. 2. As shown in the figure, there is a good agreement between these correlations and our experimental results expressed in terms of Sherwood number, *Sh*. The same figure also shows the increased mass transfer rate caused by the flow obstacles, and the increased slope of the curve, indicating a more turbulent behaviour. It is shown that the net and the cloth give the greatest enhancement of the mass transfer rate, up to ten times at the highest value of Re_a. With simultaneous axial and rotational flow, the variation of the Sherwood number was determined as a function of the Reynolds number, Re_a, for the axial flow rate and the Taylor number, *Ta*, characterizing the flow induced by the rotation. These two dimensionless numbers were varied within the ranges $39 < Re_a < 652$ and $66 < Ta < 4359$. Thus, as indicated above, laminar vortex flow was obtained in some experiments, but some experiments were also carried out in the transition flow regime ($Ta \sim 500$–1000) and in fully turbulent flow ($Ta > 1000$) [14].

The results for the smooth cylinder can be seen in Fig. 3 for $Sc = 1334$. In this figure correlations reported earlier in the literature have also been drawn for comparison. The data in this work are in good agreement with the classical results of Eisenberg *et al.* [4, 5] for rotational turbulent flow at higher values of *Ta*. For laminar flow with Taylor vortices at lower value of *Ta* the correlation obtained by Coeuret *et al.* [7–9] corresponds to somewhat lower values of the transport rate. In general, *Sh* increases with *Ta* in a way which is only weakly dependent on Re_a. However, a distinction must be made here. At low values of *Ta* and Re_a *Sh* is fairly independent of Re_a when Re_a increases. For higher Re_a number ($Re_a > 300$) at low *Ta* number, i.e. in the region where the axial flow velocity is of the same magnitude as the rotational flow velocity, *Sh* increases with increased Re_a number, whereas at higher *Ta* the dependences diminish and are equal to zero at the highest *Ta*. As for the three experiments in which the turbulence promotors were used (Figs 4–7), one can see that *Sh* increased for a fixed *Ta* number when the promotors were applied to the rotating cylinder. The increase was up to 2.1 times for the polypropene (PP) grid, 1.4–3 times for the PP net and as much as 3–6 times when the PP cloth was used. The lower value was obtained for $Ta < 500$.

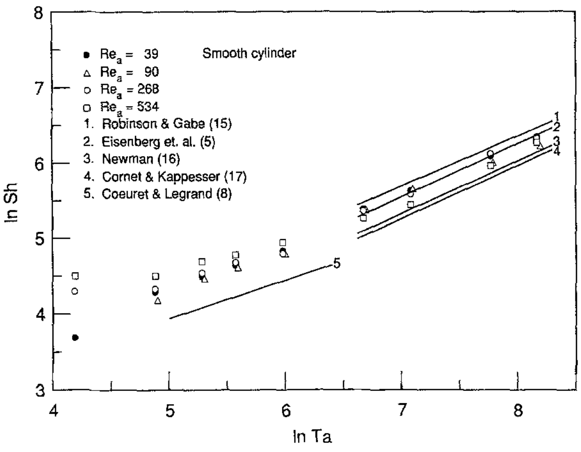

Fig. 3. Variation of Sherwood number with Taylor number and Reynolds number for a smooth cylinder ($Sc = 1334$). Comparison with correlations from the literature.

One can see in Figs 4 and 5 that for the PP net and the PP grid and for a *Ta* number less than 500 (ln $Ta = 6.2$) the *Sh* number increases when Re_a increases and the slope of the curve decreases so that at high Re_a ($Re_a > 300$) the *Sh* number is constant when *Ta* increases. This indicates that the transition zone between laminar and fully turbulent flow moves towards higher *Ta* number when axial flow, as characterized by Re_a, dominates the flow in the annulus.

For the PP cloth (Fig. 6) the *Sh* number increases when Re_a increases at $Ta < 500$ and the slope of the curve decreases but not so much. This was probably due to that fact that the flow was either in the transition region or in the turbulent Taylor vortex regime [9]. The following correlations were obtained for the

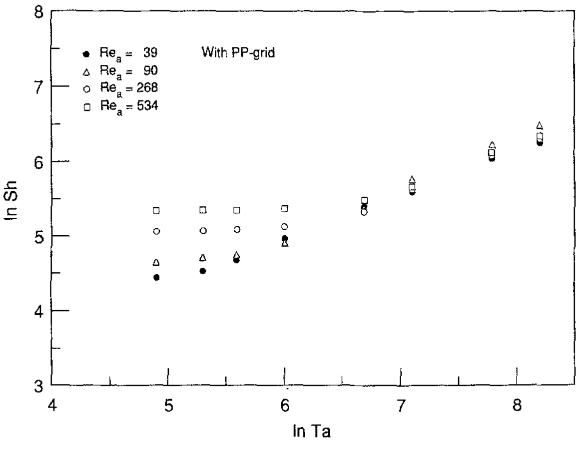

Fig. 4. Variation of Sherwood number with Taylor number and Reynolds number with PP grid as turbulence promotor ($Sc = 1334$).

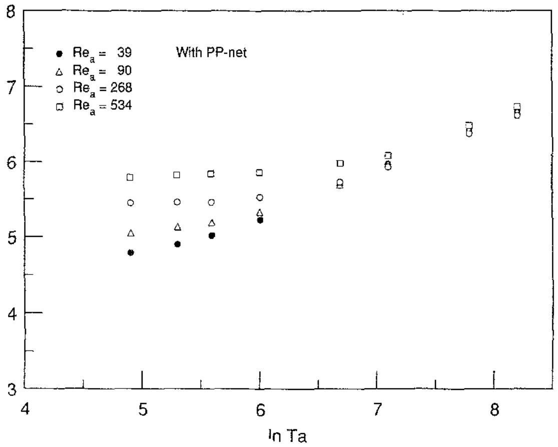

Fig. 5. Variation of Sherwood number with Taylor number and Reynolds number with PP net as turbulence promotor ($Sc = 1334$).

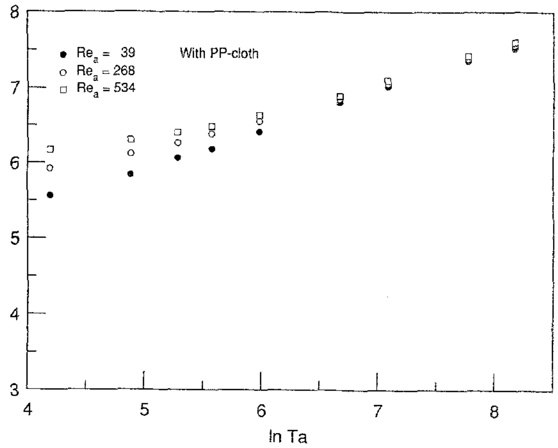

Fig. 6. Variation of Sherwood number with Taylor number and Reynolds number with PP cloth as turbulence promotor ($Sc = 1334$).

PP cloth:

$$Re_a < 100; \quad Ta \gtrsim 500: \quad Sh = 2.22 Ta^{0.51} Sc^{0.356}$$

$$100 < Re_a < 500; \quad Ta \gtrsim 500:$$

$$Sh = 3.95 Re_a^{0.1} Ta^{0.35} Sc^{0.356}$$

$$350 < Re_a < 550; \quad Ta \gtrsim 500:$$

$$Sh = 2.95 Ta^{0.48} Sc^{0.356}$$

The exponent for Sc was taken from generally accepted literature data [4, 5].

4. Discussion

The experimental results give an insight into the effects of axial flow, rotation and different turbulent promoters on the mass transfer rate to the electrode.

For the smooth cylinder, without turbulence promoters, three different regions can be distinguished with respect to the effect of rotational velocity on the rate of mass transfer to the surface of the inner rotating cylinder electrode (Fig. 3). At low Ta ($Ta \lesssim 100$) and high Re_a ($Re_a \gtrsim 200$), the value of Sh is constant with an increase in Ta and equal to the value measured at the same Re_a, but with no rotation (Fig. 2). In this region laminar axial flow alone controls the mass transport. In the intermediate region ($200 \lesssim Ta \lesssim 500$) Sh increases with Ta but is relatively insensitive to Re_a, except when going to the highest value. In this region the flow is laminar with Taylor vortices. This region has been investigated earlier by Coeuret *et al.* [7–9], who obtained somewhat lower mass transfer rates (line 5 in Fig. 3). This discrepancy may be due to a difference in cell design [1].

In the third region, for high values of Ta ($Ta > 600$), Sh increases more rapidly with increasing Ta, whereas the effect of Re_a is slightly negative. Fully turbulent rotational flow dominates. The results in this region are in good agreement with correlations reported in the literature for the rotating cylinder electrode. These correlations have been recalculated from Sh^* (rotation only) to Sh (for combined axial and rotational flow) and from Re_ω to Ta.

According to Kataoka *et al.* [14] the transition between laminar and turbulent vortex flow occurs for $Ta = 500$–1000, and the flow is fully turbulent when Ta exceeds 1000. The transition between axial flow (low Ta, high Re_a) and rotational flow (high Ta) is initiated by the generation of secondary vortices at the inner rotating electrode. This disturbance moves towards the outer stationary cylinder when Ta exceeds 1000. These phenomena were not possible to observe with the experimental equipment used and were, furthermore, not within the scope of this investigation.

The turbulence promoters change the conditions for the different flow regimes. The PP grid (Fig. 4) thus extends the region for dominating axial flow at higher values of Re_a towards higher Ta number, where transition occurs to fully turbulent, rotational flow. In this upper region the effect of the PP grid on the mass transfer rate is practicaly negligible, see Fig. 7, since full turbulence has already been reached by means of rotation.

At lower values of Ta, where axial flow dominates, the PP grid enhances the mass transfer rate by introducing a turbulent behaviour in the flow, see Fig. 2, which shows that Sh is proportional to $Re_a^{0.5}$ as in

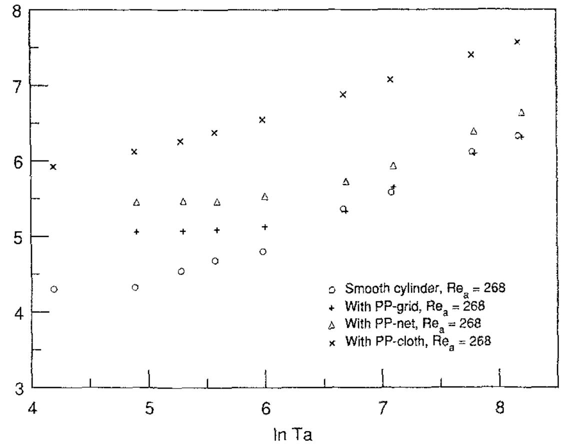

Fig. 7. Variation of Sherwood number with Taylor number at constant Reynold number ($Sc = 1334$). Comparison of turbulence promotors.

transition pipe flow. the intermediate region of laminar flow with Taylor vortices does not appear in this case, since the vortex formation is disturbed by the PP grid. For lower values of Re_a the dependence of Sh on Ta can be extrapolated from the fully turbulent region down to relatively low values of Ta, which indicates that the transition to rotational turbulent flow occurs earlier due to the turbulence promoting PP grid.

The results for the PP net (Fig. 4) can be interpreted in the same way as for the PP grid. The turbulence promoting effect is somewhat better when axial flow dominates (Figs 2 and 7). Even in the fully turbulent region the PP net gives an increase in Sh, which can be explained by the lower porosity of the packing in the annulus, which gives higher true velocities.

The PP cloth was the most efficient of the three turbulence promoters used. In axial flow with no rotation (Fig. 2) it gives no significant advantage in comparison with the PP net. With combined axial and rotational flow the PP cloth enhances the mass transfer rate considerably over the whole region investigated (Fig. 7). In contrast to the PP grid and the PP net there is no plateau in the ln Sh vs ln Ta curves for low values of Ta, but the positive effect of increasing Re_a indicates a tendency towards a plateau at even higher axial flow rates (Fig. 6).

The reason for the great effect of the PP cloth on the mass transfer rate in rotational flow is not possible to determine from the present results. A possible explanation would be that the PP cloth is in direct contact with the inner rotating cylinder electrode surface and gives a very efficient wiping effect, thereby decreasing the diffusion layer thickness.

The effect of the turbulence promoters can be measured as an enhancement factor, which is defined as the ratio between the Sherwood numbers in the presence and in the absence of the promoter. In axial flow with no rotation (Fig. 2) this enhancement factor is 1.8–2.6 for the PP grid, 2.3–4.1 for the PP net and 2.9–4.4 for the PP cloth. The lower values are for $Re_a = 37.7$. In fully turbulent flow ($Ta < 1000$) the enhancement factor is 1.0 for the PP grid, 1.4 for the PP net and 3.5–4.6 for the PP cloth (Fig. 7).

5. Conclusion

When the turbulence promotors were applied in the annulus a significant increase in Sh was detected, up to five times the value for the smooth cylinder when the PP cloth was used. The very high mass transfer rates should be useful in practical applications such as the removal of heavy metal ions from dilute waste waters.

Acknowledgements

This work was financially supported by the National Swedish Board for Technical Development (STU). Valuable discussions with Professor Fritz Bark, Mr Martin Bursell and Dr Hans Medin are gratefully acknowledged.

References

[1] D. R. Gabe and F. C. Walsh, *J. Appl. Electrochem.* **13** (1983) 3.
[2] D. J. Picket, 'Electrochemical Reactor Design', Elsevier, Amsterdam (1977).
[3] D. R. Gabe, *J. Appl. Electrochem.* **4** (1974) 91.
[4] M. Eisenberg, C. W. Tobias and C. R. Wilke, *Chem. Eng. Progr. Symp. Ser.* **51** (1955) 1.
[5] M. Eisenberg, C. W. Tobias and C. R. Wilke, *J. Electrochem. Soc.* **101** (1954) 306.
[6] D. R. Gabe and D. J. Robinson, *Electrochim. Acta* **17** (1971) 1129.
[7] F. Coeuret and J. Legrand, *Electrochim. Acta* **28** (1983) 611.
[8] F. Coeuret and J. Legrand, *Electrochim. Acta* **26** (1981) 865.
[9] J. Legrand, P. Dumargue and F. Coeuret, *Electrochim. Acta* **25** (1980) 669.
[10] D. R. Gabe and P. A. Makanjuola, *J. Appl. Electrochem.* **17** (1987) 370.
[11] A. J. Arvia, S. L. Marchiano and J. J. Podesta, *Electrochim. Acta* **12** (1967) 259.
[12] 'Handbook of Chemistry and Physics', 53rd edn, CRC Press (1972–1973).
[13] T. K. Ross and A. A. Wragg, *Electrochim. Acta* **10** (1965) 1093.
[14] K. Kataoka, H. Doi and T. Komai, *Int. J. Heat Mass Transfer* **20** (1977) 57.
[15] D. J. Robinson and D. R. Gabe, *Trans. Inst. Metal Finishing* **48** (1970) 35.
[16] J. Newman, 'Electrochemical Systems', Prentice-Hall, Englewood Cliffs, New Jersey (1973).
[17] I. I. Cornet and R. R. Kappesser, *Trans. Inst. Chem. Engrs* **47** (1969) T194.